diffusion-fundamentals

The Open-Access Journal for the Basic Principles of Diffusion Theory, Experiment and Application

Molecular Diffusion under Confinement

Jörg Kärger

Universität Leipzig, Fakultät für Physik und Geowissenschaften, Germany
E-Mail: kaerger@physik.uni-leipzig.de

Abstract

With reference to molecular transport in manifold media of porous structure, a survey is given on the ample spectrum of diffusion phenomena under confinement. The presentation is mainly based on the evidence provided by pulsed field gradient NMR and by interference and IR microscopy. These "microscopic" techniques of diffusion measurement are particularly powerful for exploring the diverse features of molecular propagation in complex systems. The presented data cover the peculiarities of molecular diffusion under the regime of "intracrystalline" zeolitic diffusion, refer to deviations from normal diffusion and deal with the practically particularly important case where the overall diffusion process includes molecular propagation in the gas phase. In many cases, the reported experimental studies have been performed in immediate response to theoretical issues including single-file diffusion and sorption hysteresis. Simultaneously, they have given rise to new challenges for basic research correlating equilibrium and non-equilibrium phenomena of molecular propagation.

key words: pulsed field gradient NMR, interference and IR microscopy, anomalous diffusion, hysteresis, tortuosity, single-file diffusion, zeolites, sorption kinetics

1. Introduction

Adolf Fick's [1] and Albert Einstein's [2] pioneering work on diffusion dealt with homogeneous fluids, so that still today, 150 and 100 years after their seminal papers, diffusion is often understood as a phenomenon exclusively related to homogeneous media. This restriction, however, does only hold in relation to the observed displacements and the correlation length of sample heterogeneity. There is probably no doubt that even in fluids the famous Fick's first and second laws

$$j_x = -D\frac{\partial c}{\partial x} \tag{1}$$

$$\frac{\partial c}{\partial t} = D\frac{\partial^2 c}{\partial x^2} \tag{2}$$

for the flux density j_x and the change in local concentration c, respectively, and the celebrated Einstein relation (following from eq.(2), for an initial concentration $c(x, t=0)$ equal to Dirac's delta function $\delta(x)$, as the variance of the concentration distribution)

$$\langle x^2(t)\rangle = 2Dt \tag{3}$$

between the root mean square displacement and the observation time - for simplicity, noted here for the one-dimensional case only - do not hold unrestrictedly. One has rather

to require that the considered displacements x, the volumes to which the concentrations c are referred, and the observation times t are large in comparison with the intermolecular distances, their cubes and the mean time to travel over these distances, respectively.

Today, technological progress in many areas has led to the fabrication of many highly structured, "complex" media. It is just this deviation from homogeneity which features their functionality. The present contribution will particularly deal with porous media, whose functionality most decisively depends on the size, dispersion and connectivity of the pores. Prominent examples for the application of such materials include mass transformation by heterogeneous catalysis [3, 4] and mass separation by membranes [5] and selective adsorption [6]. Obviously, mass transfer in also these materials may appropriately be described by eqs. (1) to (3) if only the space and time scales considered are sufficiently large in comparison with the pore sizes (or the correlation lengths of a given pore hierarchy) and the mean time it takes a molecule to cover these distances.

Our present understanding of the transport properties within such porous materials has highly benefited from the special insights allowed by the pulsed field gradient (PFG) NMR technique. The fundamentals and procedure of PFG NMR (often also referred to as PGSE (pulsed gradient spin echo) technique) are described in many textbooks [7-9] and review articles [10-12] and are referred to in more detail in this volume in the contributions by Paul Heitjans and William S. Price. The principle of PFG NMR is closely related to Magnetic Resonance Imaging (MRI) which in the last decade has attained the top position among the imaging techniques of medical diagnosis [7, 13, 14]. While the latter uses the NMR signal to record particle positions (thus providing the image of the given part of the human body), PFG NMR compares the position of each particle within two subsequent instants of time. This, as the final output of PFG NMR, results in the probability distribution of molecular displacements within the sample under study, the so-called mean propagator [7, 15, 16]. The observation times and observable displacements are on the order of milliseconds and micrometers, respectively. The probability distribution of molecular displacements is often (viz. in the case of "normal" diffusion) completely described by its mean square displacement as provided by the Einstein relation, eq. (3).

Typically, the PFG NMR measurements are performed under equilibrium conditions. Molecular transportation recorded under such conditions is generally referred to as self- or tracer diffusion. Conventionally, i.e. before the advent of PFG NMR, the relevant parameters of self- or tracer diffusion had to be determined by isotopic labeling. In this case, the concentration in eqs.(1) and (2) refer only to the labeled component.

As a most astonishing result of the early days of PFG NMR [9, 17, 18], for a number of systems the data on intracrystalline self-diffusion in zeolites, a particularly important class of nanoporous crystallites [19-21], were by orders of magnitude larger than generally assumed up to this point on the basis of uptake or release measurements. In this latter type of experiments one observes the rate of the change of overall molecular concentration in a batch of zeolite crystallites after having reduced (in release experiments) or enhanced (in uptake experiments) the pressure in the surrounding gas phase. Information about intracrystalline diffusion is then deduced by fitting the solution of eq.(2) under the appropriate initial and boundary conditions to the experimental data.

In most of these systems the discrepancy could be explained by realizing that very often external effects of transport limitation like the exchange of the heat generated during the adsorption or consumed during the release experiments, the molecular transport through the bed of crystallites and/or the rate of molecular exchange between the sorption vessel and the surroundings (due to "valve" effects) rather than intracrystalline diffusion represented the rate-controlling processes [9, 22-25]. There were, however, also a number of well-documented experiments with discrepancies between the uptake/release and PFG NMR studies, where all these explanations could be excluded.

It was due to this reason that, in addition to PFG NMR - a microscopic technique operating under equilibrium conditions - , interference microscopy [26-28] and IR microscopy [29] have been introduced. From an analysis of the intensity of an appropriate IR band or of the change in the optical density of a zeolite crystal, these techniques are able to monitor microscopically the changes of intracrystalline concentration profiles. They are thus microscopic techniques operating under non-equilibrium conditions. The quantity directly measured is the integral of the local concentration (referred to an *x*-*y*-plane element of 1×1 μm^2 in interference microscopy and of (presently) 20×20 μm^2 in IR microscopy) in observation direction through the crystal.

Further details of these techniques and their application may as well be found in the review [30]. In the following, the mutual benefit of both techniques, in particular for elucidating the real structure of nanoporous materials and their consequence for the intrinsic phenomena of mass transfer, shall be displayed. The subsequent section 2 will demonstrate how the real structure of zeolite particles, i.e. their deviation from the textbook pattern, may disguise the real scenario of intracrystalline molecular transportation. In section 3 we shall discuss experimental prerequisites under which the observation of deviations from normal diffusion over longer, well-defined intervals of time may become feasible. Finally, section 4 will deal with the peculiarities of molecular transportation if it comprises different modes of propagation including gas phase diffusion.

2. Micropore Diffusion and the Influence of the Real Structure of Zeolites

2.1 Intracrystalline Transport Resistances

PFG NMR has been established as a highly reliable and versatile technique for the measurement of intracrystalline zeolitic diffusion [9, 31]. In order to ensure that the obtained diffusivities are in no way affected by the finite size of the zeolite crystallites or by the transport in the intercrystalline space, the observation times (this is the time between the two gradient pulses) have to be chosen small enough so that molecular displacements remain negligibly small with respect to the crystal sizes. If this condition cannot be perfectly met, a formalism derived by Mitra et al. [32, 33] may serve as an excellent means for checking the influence of the finite crystal size in first-order approximation. In [34], this formalism has been shown to exactly reflect the boundary conditions exerted by the crystal surface on the measurement of intracrystalline diffusion for n-hexane and tetrafluoromethane in zeolite NaX.

In view of this ideal correspondence between the measured ("effective") diffusivities and the crystal sizes, the finding with n-butane in zeolite crystallites of type silicalite-1 [35, 36], as displayed by fig. 1, deserves particular concern.

In fig. 1 the diffusivity data are plotted in a way, which is made possible by the special features of PFG NMR, viz. as a function of the displacements over which the molecular diffusion paths giving rise to the plotted diffusivities have been measured. This is achieved on the basis of eq. (3) by which the measured diffusivities may be transferred into the mean square displacements covered by the molecules during the observation time. Obviously, in the case of ordinary diffusion, i.e. in the original notion of eq. (3), the diffusivity depends on neither the observation time nor the displacements. However, eq. (3) has turned out to be a reasonable relation for introducing "effective" diffusivities, reflecting the transport properties also under conditions deviating from those for normal diffusion.

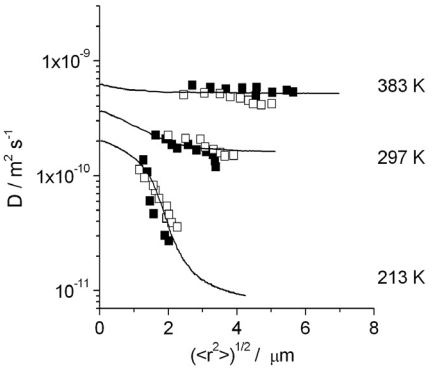

Fig. 1. Dependencies of the diffusion coefficients of n-butane in silicalite-1 on the root mean square displacements at different temperatures and comparison with the results of MC simulations for a barrier separation of 3 μm with the assumption that jumps across the barriers occur with an activation energy exceeding that of intracrystalline diffusion by 21.5 kJ/mol. Filled and open points correspond to the measurements performed with two different samples of silicalite-1.

In the above-mentioned Mitra formalism [32, 33] and its application to zeolites in [34], these deviations may be referred to the size of the individual crystallites. In the studies of ref. [36], however, crystallites of such large extension (100×25×20 μm^3) have been applied, so that only for displacements notably larger than 10 μm the crystallite surfaces might have given rise to such a steep decay as observed at the lowest temperatures.

As the - as to our knowledge - only explanation of this behaviour one has to require that there are extended intracrystalline transport resistances (internal barriers), giving rise to the observed dependence of the effective diffusivities on the covered displacements. Obviously, at the highest temperature the thermal energy of the diffusing molecules is high enough to overcome these barriers so that their influence becomes negligibly small in comparison with the transport resistance due to the genuine pore system. The solid lines show the results of dynamic Monte Carlo simulations with the assumption that, in addition to the energetic barrier characterising diffusion in the genuine intracrystalline pore system, at a distance of 3 μm, the diffusing molecules have to overcome additional potential barriers of 21.5 kJ/mol [35]. It is remarkable that the anomaly of the PFG NMR data may be satisfactorily explained already by such a rather simplistic model.

The evidence of the PFG NMR data nicely confirms the conception of the possible existence of intracrystalline transport barriers, which has been suggested as one of the possibilities to explain the discrepancy in the results between different techniques of diffusion measurement on zeolites [37]. The occurrence of such barriers is not unexpected, judging from both the concepts of crystal formation [38, 39] and the existence of distorted terraces on the surface of such crystallites [40]. Their direct structural demonstration, however, has to remain a task for the future.

2.2 Disguised Sorption Kinetics

In addition to the resulting time constant, the information deduced from conventional uptake and release experiments on intracrystalline diffusion was in particular based on the observed time dependence. It may be easily rationalized that in its initial part molecular uptake should be proportional to the square root of time if the overall process is limited by intracrystalline diffusion. Let us consider molecular uptake by an initially empty crystal. As a first estimate, the total amount of molecules having penetrated into the crystal after time t may be assumed to be given by the intracrystalline concentration close to the surface (which is assumed to be the value in equilibrium with the surrounding atmosphere) times the total crystal surface times the mean diffusion path length of the molecules (the product of the latter two factors representing an approximation of the part of the crystal accommodating already at the given instant of time sorbate molecules). With eq.(3) one thus immediately obtains the so-called $\sqrt{t}$-law of diffusion-limited sorption.

Being able to directly unveil the prevailing transport phenomena during molecular uptake or release by interference microscopy, one may test the reliability of such a so far quite generally accepted criterion for the underlying mechanisms. This section provides a short review of the representation in ref.[41]. It is based on extensive studies of the ad- and desorption of methanol on crystallites of ferrierite. Let us refer to the example given in fig. 2.

The ferrierite crystals used in this study consisted of platelet-like crystallites, as schematically shown on the bottom of fig. 2a. Remarkably, the crystals turned out to be of double-roof shape rather than an ideal plate. From x-ray diffraction analysis, ferrierite crystals are known to be traversed by two sets of parallel channels, one being formed of so-called 10-membered rings (consisting of 10 oxygen atoms with silicon in between) parallel to the longitudinal extension, i.e. in z direction, and the other one in y direction, consisting of 8-membered rings.

The measurement of concentration profiles and of their evolution as shown in the upper part of fig. 2a has become possible by interference microscopy and is brand new. We may deduce from it the following remarkable features:

(i) In a fast, first process (with a characteristic time constant of notably less than 30 seconds) the roof-like part of the crystals is filled. This might be associated with the fact that in this part the 10-membered ring channels are easily accessible owing to their very large orifices.

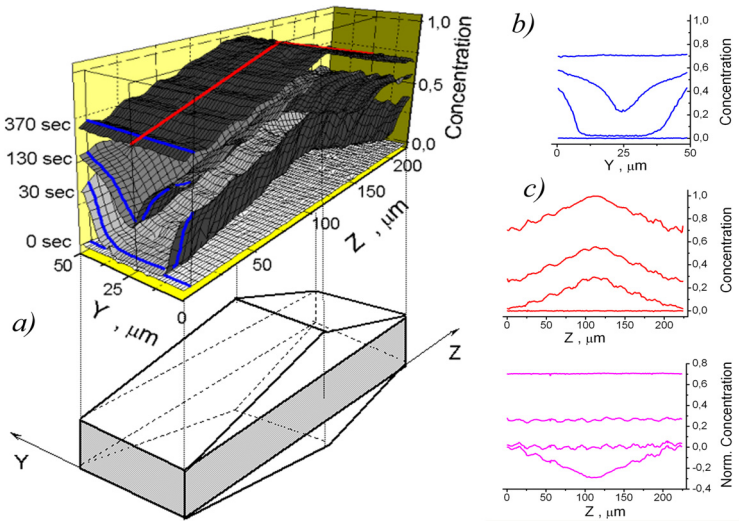

Fig.2. Shape and dimensions of the ferrierite crystal and 2D-concentration profiles for the entire crystal (a) and concentration profiles during methanol adsorption in (b) the *y*-direction near the crystal edge, *z*=2 µm, fat black line in the profiles of Fig. 2(a), and in (c) the *z*-direction in the middle part of the crystal, *y*=25 µm (top), measured by interference microscopy for pressure step 0 → 80 mbar. The normalized concentration profiles along *z*-direction derived by substracting the "roof-like" profile are also shown (bottom). The shown profiles were measured at the same times after the start of adsorption.

(ii) In addition, mass transfer into *z* direction (i.e. in the direction of the large channels) occurs so fast that the apparent concentration gradient in *z* direction (top of fig. 2c) is exclusively brought about by the linearly increasing thickness of the crystal towards its central part (comparison figs. 2c top and bottom)

(iii) Not unreasonably, mass transfer into *y* direction, i.e. along the narrower channels, proceeds at a notably lower speed. It is possible, therefore, that the evolution of intracrystalline concentration profiles may be followed (fig. 2b).

(iv)The curved concentration profiles in the direction of the narrow channels unambiguously indicate the existence of some diffusion resistance. However, molecular uptake is still found to be as well determined by notable surface resistances. Otherwise the concentration profiles in fig. 2 b should attain their equilibrium values at the crystal boundary (i.e. for $y = 0$ and 50 µm) immediately after the onset of uptake.

(v) Irrespective of the fast rate of molecular propagation along the broader channels, it takes a notable period of time, up to some hundreds of seconds, until the whole crystal is filled. This indicates the existence of substantial surface barriers on the face surfaces ($z = 0$ and ≈ 220 µm).

Interference microscopy is thus found to provide an impressive, detailed record on the variety of transport phenomena relevant for molecular uptake (as well as for molecular release) of methanol for the ferrierite-type zeolites under study. It is important to note that the sole representation of the total uptake as resulting by either a simple integration over all the total concentration profile as well as by parallel single-crystal studies of

molecular uptake and release by IR microscopy [41] leads to a time function which much better fits to the $\sqrt{t}$ dependence, characteristic of diffusion-limited sorption, than to barrier-limited uptake, which interferences microscopy unambiguously identifies as the dominating mechanism.

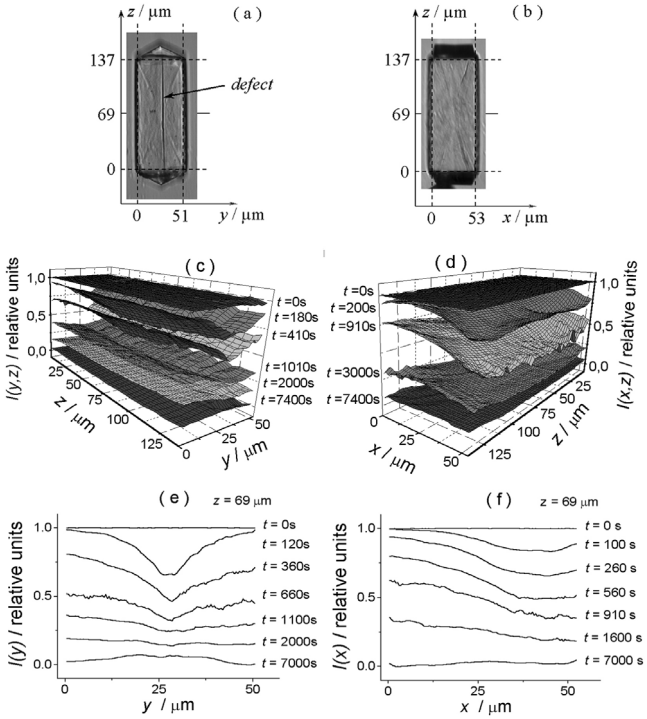

Fig.3. Microscopic images of the crystal and intracrystalline concentration profiles of isobutane recorded by interference microscopy during the desorption of isobutane in nonetched ZSM-5 crystals. The observation direction was perpendicular to the (z,y) plane in parts a, c. and e and perpendicular to the (z,x) plane in parts b, d, and f. The desorption was initiated by a rapid change of the isobutane pressure in the cell from 10 to 0 mbar. The concentration integrals I=1.0 correspond to those measured under equilibrium with an isobutane pressure of 10 mbar. The t values shown in parts c-f indicate the time intervals after the start of desorption.

Fig.3 may serve as another example of the surprising details of molecular sorption which may be revealed by interference microscopy [42]. Figs. 3 c and d show the profiles of integral concentrations during the desorption of isobutane from a zeolite crystallite of type ZSM-5. The direction of integration (coinciding with the direction of observation, i.e. the directions perpendicular to the images shown in figs. 1a and b) are the x (fig. 3c) and y (fig. 3d) axes, respectively. The cuts at z = 69 µm (fig. 3e) in the profiles (fig. 3c) observed in x direction reveal the remarkable fact that desorption is fastest in the central part of the crystal, i.e. for $y \approx 25$ µm. Again, such a behaviour is incompatible with our conventional understanding of molecular uptake and release on zeolites: Since the molecules are assumed to leave the crystallites through the external surface, their

concentration has to decline from inside to outside, with a constant profile in the case of dominating surface barriers. In the present case, however, a crack in the crystal structure ensures fast molecular penetration into the crystal in just this central range. Such cracks, which have been found to be quite common for these larger zeolite crystallites [42], most likely emerge during the crystal calcination as a consequence of internal tensions. This assumption corresponds with the fact, that these cracks were found on only one crystal face. Having this fact in mind, a second surprising feature, viz. the asymmetry in the concentration profiles observed during desorption with the crystal turned by 90° (figs. 3 d and f) becomes immediately understandable.

Unveiling intracrystalline diffusion in nanoporous materials has thus become a truly interdisciplinary task representing challenges for most diverse areas of research. They include the synthesis of ideal, well-shaped and hopefully large zeolite crystallites, their minute structural characterization, the continued improvement and further development of the experimental techniques of diffusion measurement under the given conditions and, last not least, close contact with theoretical concepts for correlating the different conditions under which molecular diffusion in such systems may be measured.

3. Anomalous Diffusion

The preceding section was thought to demonstrate that the reliable observation of such an apparently simple phenomenon like normal diffusion in nanoporous materials is by far not trivial and a hot topic of current research. It is, however, already now justified to accept the continuative challenge of investigating under which experimental conditions molecular transport in porous media might give rise to such well-defined deviations from normal diffusion which allow their discussion in terms of the conception of anomalous diffusion, i.e. by implying that the proportionality

$$\langle x^2(t)\rangle \propto t^{\kappa} \text{ with } \kappa \neq 1 \qquad (4)$$

is obeyed over a notable range of displacements and observation times [9, 43, 44]. In the following, we are going to present two cases where PFG NMR has nicely reflected this dependence.

3.1 Porous Polymer Membranes

The strict periodicity of crystalline nanoporous materials like zeolites gives rise to proportionality between the mean square displacement of the guest molecules and the observation time as soon as the observed mean diffusion paths exceed the size of the elementary cells. Incidental deviations from the ideal structure, as discussed in section 2.1 as the origin of the diverging messages of different techniques of diffusion measurement, clearly lead to deviations from this pattern. But they fail to give rise to conditions under which molecular propagation is found to follow eq.(4) over significant ranges of displacement and observation

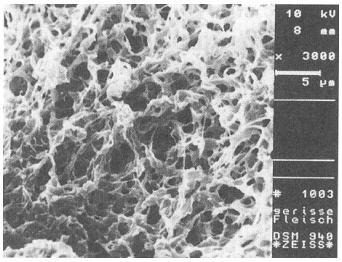

Fig. 4. Scanning electron micrograph of the porous polypropylene matrix used in the experiments. The visible structures larger than about 1 µm are artefacts due to the probe preparation.

times with one and the same value of κ [45]. Measurements of this type imply some hierarchy and self-similarity of the pore structure.

PFG NMR diffusion measurements with appropriately chosen guest molecules (polydimethylsiloxane (PDMS) with a molecular weight of 22530 g/mol) in a commercially available porous polymer membrane of Type Accurel [46] turned out to reveal anomalous diffusion. Fig. 4 shows a scanning electron micrograph of the polymer membrane which displays the inherent pore size distribution. Fig. 5 provides a complete survey of the diffusivities observed at total pore filling, plotted in the way of fig. 1, i.e. as a function of the covered molecular displacements. In this representation, the PFG NMR data are complemented by the values obtained by diffusion measurements in the stray field of a superconducting magnet (SFG NMR) which allows the observation of even smaller displacements [47-49].

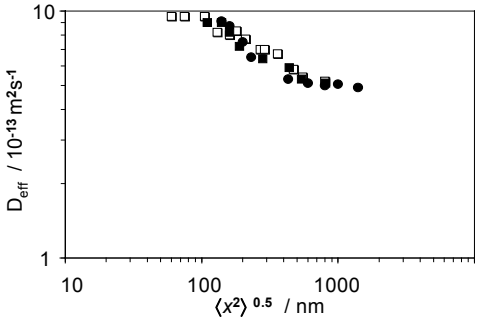

Fig.5. Effective diffusivity of PDMS (M_W=22530 g/mol) in a polypropylene host matrix at a pore filling factor of 100 % at 293 K as a function of the root mean square displacement of PDMS during the NMR experiment. The filled circles refer to effective diffusivities extrapolated from measurements at 343 K to room temperature. The open symbols are data of SFG NMR, the filled symbols are data of PFG NMR.

One may easily identify the two limiting cases in which molecular propagation is found to obey ordinary diffusion, i.e. to yield a diffusivity independent of the covered displacements. For sufficiently short observation times the displacements could be reduced to values smaller than the smallest pore diameters, which ranged from about 200 nm up to about 650 nm, so that the diffusivities approached those of the guest polymers in their pure liquid phase. It is interesting to note that for displacements on the order of the largest pore diameters again a constant value of the diffusivities is attained, which is now reduced by the effect of the pore network. In between these two limiting cases, there is the range of effective diffusivities which vary with the displacements covered during the observation time and hence with the observation time itself.

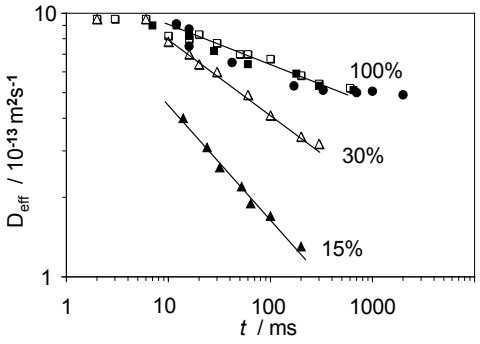

Fig. 6. Effective diffusivity of PDMS (M_W=22530 g/mol) in a polypropylene host matrix at pore filling factors as indicated. Open symbols refer to SFG NMR, filled symbols to PFG NMR.

Fig. 6 shows the thus resulting time dependence of the effective diffusivities for three different pore filling factors. It appears that the deviation from ordinary

diffusion, i.e. from a diffusion coefficient constant in time, becomes more pronounced with decreasing pore filling factor. Since the polypropylene matrix is easily wettable by PDMS, this is exactly the behavior one has to expect: With decreasing loading, PDMS will more and more form a thin film along the internal surface of the host matrix. In this way, PDMS becomes even more sensitive to the structural confinement exerted on it by the host matrix. From a topological point of view, molecular diffusion is now more likely to proceed under the influence of a surface fractal rather than a pore fractal [50-52]. Via eq. (3), these diffusivities may be transferred into the corresponding mean square displacements from which - by comparison with eq. (4) - the time exponents of anomalous diffusion are found to be $\kappa = 0.83$, 0.72 and 0.55 for the pore filling factors 1, 0.3 and 0.15, respectively.

3.2 Nanoporous Crystals with 1d-Channel Arrays

For a substantial number of zeolites, including ZSM-12, -22, -23, -48, $AlPO_4$-5, -8, -11, L, Omega, EU-1 and VPI-15 [19], the intracrystalline pore system is found to consist of an array of parallel channels. As soon as the diameters of the guest molecules notably exceed the channel radii, their mutual passage is prohibited so that the molecules within each individual channel have to maintain their order. Molecular transport under such confinement - viz. the one-dimensional stochastic movement of particles with hard-core interaction - is referred to as single-file diffusion.

By the very nature of this process, in an infinitely long single-file system subsequent displacements do never loose their mutual correlation: The farther a molecule is shifted in a given time interval into one direction, the larger is the probability that, in a subsequent interval of time, this molecule is shifted into the opposite direction. This is a simple consequence of the fact that under single-file constraint, on the average, molecular shifts are accompanied by concentration enhancement "in front" of the molecule and by concentration decrease behind it.

In a few lines this situation may be rationalized to lead to anomalous diffusion, i.e. to a deviation from eq. (3). Let us consider molecular displacement $x(t)$ as the sum of the displacements $(\Delta x)_i$ during the time intervals $(\Delta t)_i$ (with $t = \sum (\Delta t)_i$). Then, the mean square displacement $<x^2(t)>$ results as the sum of all possible products $<(\Delta x)_i(\Delta x)_j>$. If subsequent displacements are uncorrelated, for a given value of $(\Delta x)_i$, the values of $(\Delta x)_j$ (for $i \neq j$) shall be equally often positive and negative so that all cross terms vanish. Hence, the mean square of the sum of displacements is equal to the sum of the mean squares of the displacements, so that the total mean square displacement increases in proportion to the number of time intervals, i.e. to the total observation time. This is the well known scenario of normal diffusion.

Under the just discussed conditions of single-file diffusion, subsequent displacements $(\Delta x)_i$ are most likely of different sign. As a consequence, on calculating the mean square of the displacement sum, in addition to the sum of the squares of the individual displacements, the cross terms $<(\Delta x)_i(\Delta x)_j>$ with $i \neq j$ will lead to a negative contribution and hence to the tendency that the total mean square displacement increases less than linearly with increasing observation time.

Rigorous analysis [53-55] leads to proportionality with but the square root of the observation time

$$\langle x^2(t)\rangle = 2Ft^{1/2} \qquad (5)$$

where - assuming propagation by jumps of length l with a mean residence time τ between subsequent jumps - the factor of proportionality is found to obey the relation

$$F = l^2 \frac{1-\theta}{\theta}\frac{1}{\sqrt{2\pi\tau}}. \qquad (6)$$

It is interesting to note that - irrespective of the completely different time dependence of the mean square displacement - also under single-file conditions the probability distribution of the displacements is given by a Gaussian - now, instead of eq.(3), with the root means square displacement given by eqs.(5) and (6)[56, 57].

Fig.7. Unconventional way of testing single-file diffusion in the great lecture hall of the Physics Department of the Leipzig University: The students generate their "random walk" by throwing coins. Depending on the result they switch to one of the neighbouring seats, provided it is vacant.

A rather unconventional way of testing single-file diffusion is shown in fig. 7. Here, students in the great lecture hall of the Physics Department of the Leipzig University generate their "random walk" by throwing coins. Depending on the result they switch to one of the neighbouring seats, provided it is vacant.

In Lothar Riekert's pioneering paper on the interrelation between sorption, diffusion and reaction in zeolites [58] for the first time molecular propagation in zeolites has been discussed in terms of single-file diffusion. It was, however, not before 1992 when first predictions on diffusion and reaction in zeolites of 1d-channel structure [59] initiated an ongoing, extensive investigation of single-file diffusion and reaction in zeolites. It comprises theoretical activities including analytical approaches [60-67], dynamic Monte Carlo simulations [68-71] and Molecular Dynamics [72-79]. Experimental studies have been devoted to both the catalytic conversion under single-file conditions [60, 80-86] and diffusion measurements by PFG NMR [49, 87-91] and Quasi-Elastic Neutron Scattering [92]. Independently from each other, in [87] and in [88-90]

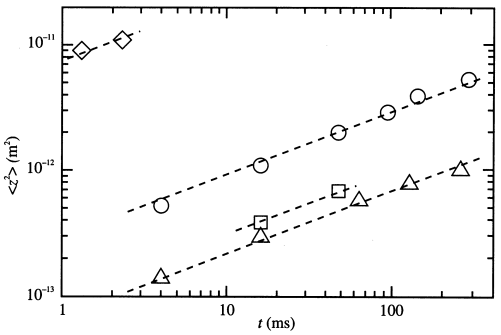

Fig. 8. Molecular mean square displacement of CF_4 in $AlPO_4$-5 at 180 K as a function of the observation time at a sorbate concentration of 0.005 (◊), 0.05 (○), 0.2 (□)and 0.4 (Δ)

by PFG NMR the molecular mean square displacement in a number of zeolitic adsorbate-adsorbent systems, whose internal text-book geometry should have been expected to yield single-file conditions, was found to increase in proportion with the square root of time (eq.(5)) rather than with the time itself.

As an example, fig. 8 shows the molecular mean square displacement of CF_4 in a zeolite of type $AlPO_4$-5 as a function of the observation time for different pore filling factors θ. It turns out that both the time dependence (as immediately visible from the representation) and the dependence on the pore filling factor are in satisfactory agreement with the behaviour expected on the basis of eqs.(5) and (6).

However, before this coincidence can be taken as an unambiguous indication that single-file confinement did in fact lead to the observed time dependence, two very important problems are still to be clarified. First, one has to be aware of the fact that even in an ideal single-file system eq.(5) does only unrestrictedly hold if the system is infinitely extended. Real zeolite crystals, however, have a finite size. Hence, molecular exchange at the crystal boundaries may give rise to a stochastic movement of the whole file of molecules (a "centre-of-mass" diffusion), which is superimposed to the displacement of each individual molecule with respect to the file. Since subsequent processes of molecular adsorption or desorption on the marginal sites tend to occur independently from each other, the process of displacement due to this mechanism follows the laws of normal diffusion with an effective diffusivity [68-70, 93]

$$D_{\mathrm{eff}} = D\frac{1-\theta}{\theta N}. \qquad (7)$$

Here, D ($\equiv l^2/2\tau$) denotes the self-diffusivity of an isolated molecule in the file and N ($= L/l$, with file length L) stands for the number of sites. Comparing eqs.(5) (with F given by eq.(6)) and (3) (with D given by eq. (7)) one obtains as the cross-over value from single-file to normal diffusion a mean square displacements of

$$\langle x^2 \rangle_c = \frac{2}{\pi}\frac{1-\theta}{\theta} Ll. \qquad (8)$$

Thus one finds that even for the particularly large zeolite crystals of lengths up to 200 μm, as considered in [68-70, 93], the cross-over from the single-file time dependence (eq. (5)) to that of normal diffusion (eq.(3)) should become visible for the displacements observed and shown in fig. 8.

This, however, can only be expected to occur if the intracrystalline channel system of the zeolites under study may in fact be considered as the analogue of a bundle of macaronis with atomistic dimensions.

So far, however, such unequivocal structural evidence could not be provided [29, 30, 94, 95]. In fact, in those cases were the channel filling of zeolites with supposed single-file structure could unambiguously be monitored, notable deviations from the ideal behaviour was observed. As an example, fig. 9 shows the result of such an experiment, recording the equilibrium concentration of methanol in a CrAPO-5 crystal which, among the possible candidates for single-file type structures, are distinguished owing to their high crystallinity [96-98]. Though the crystal structure is known to consist of hexagonally arranged channels in z direction (fig. 9d), the concentration profiles observed by interference microscopy (IFM) both in y direction (fig. 9a, view perpendicular to one of

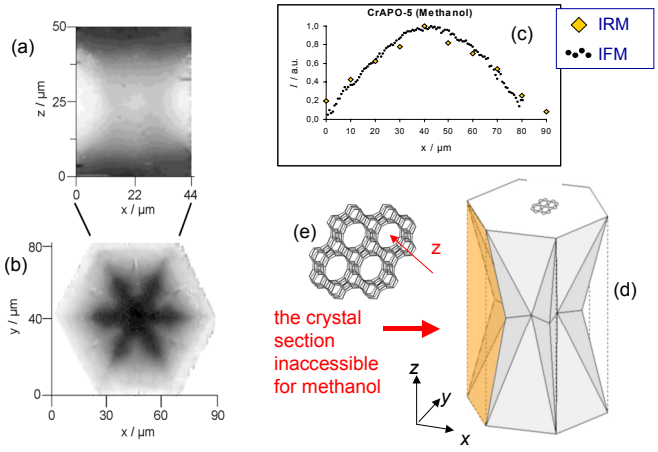

Fig.9. Equilibrium intracrystalline concentration profiles of methanol in a CrAPO-5 crystal: 2d-profiles of mean concentration for observation perpendicular to one side face (a) and along axis direction (b) (the colour intensity is proportional to the mean concentration), comparison between interference data (taken from (b)) and IR data for the concentration profile in x direction with y values between 35 and 55 µm (c) and derived structure model (d) substantiating the text-book structure model (e).

the six prism faces) and z direction (fig. 9b, view along the axis of sixfold symmetry) indicate significant deviations. With a correspondingly smaller spatial resolution, the results of interference microscopy are reproduced by IR microscopy (IRM, fig. 9c). The structure model deduced from these profiles (fig. 9d) notably deviates from the bundle-of-macaronis conception.

Thus, the synthesis of crystalline nanoporous materials offering the structure of an ideal host for single-file systems seems to remain a challenging task for the future.

4. Diffusion Traversing the Gas Phase

Some special features of molecular diffusion under confinement are the consequence of an interchange between different regimes of molecular propagation. In the following, we shall confine ourselves to the special case, where molecular diffusion under confinement changes with periods, where molecular propagation proceeds in the free space. In general, observation of such phenomena by PFG NMR occurs under the conditions of fast exchange. This means that the observation time is long enough to ensure that the diffusing molecules sufficiently often exchange between the different regimes of propagation. In this case, the effective diffusivity as observed by PFG NMR simply results as a weighted superposition of the diffusivities under the different regimes of propagation [10, 99-101] (see also the contribution by W. S. Price to this volume)

$$D_{\mathrm{eff}} = \sum p_{\mathrm{i}} D_{\mathrm{i}} \,, \qquad (9)$$

where p_{i} denotes the relative number of molecules which, at a given instant of time, are within a regime of diffusivity D_{i}. We shall consider two cases, viz. molecular

diffusion through a bed of zeolite crystallites in section 4.1, and, in section 4.2, molecular diffusion through mesopores. In the latter case we shall be concerned with the rates of molecular propagation both on the pore surface and through the gas phase. Particular attention shall be given to the influence of phase transitions within the pores on molecular propagation.

4.1 Diffusion through beds of zeolites: the effect of tortuosity

The influence of intracrystalline molecular displacements on the overall transport through beds of zeolite crystallites is negligibly small so that eq.(9) simplifies to [9, 102]

$$D_{\text{eff}} = D_{\text{long-range}} = p_{\text{inter}} D_{\text{inter}} \tag{10}$$

where p_{inter} and D_{inter} denote, respectively, the relative amount of molecules in the intercrystalline space, i.e. in the gas phase between the crystallites, and their diffusivity.

As an example, fig. 10 displays the thus determined ("long-range") diffusivity of ethane in a bed of crystallites of zeolite NaX [103]. For rationalizing the observed dependence one has to recollect that the diffusivity in the gas phase may be estimated by the simple gas-kinetic approach [9, 104, 105]

$$D_{\text{inter}} = \frac{1}{3} \lambda_{\text{eff}} u / \tau \tag{11}$$

where λ_{eff}, u and τ respectively denote the mean free path, the thermal velocity and the tortuosity of the intercrystalline space. At sufficiently low temperatures the gas phase concentration is so small that within the intercrystalline space mutual encounters of the molecules essentially do not occur (Knudsen diffusion, insert on the right). Therefore, the effective mean free path λ_{eff} in eq. (11) is given by the mean diameter of pores formed by the intercrystalline space. Thus, having in mind that the thermal velocity u increases only with the square root of temperature, the temperature dependence of $D_{\text{long-range}} = p_{\text{inter}} D_{\text{inter}}$ is essentially given by that of p_{inter}. Since the relative concentrations in the gaseous and adsorbed phases are interrelated by the Boltzmann factor one has $p_{\text{inter}} \propto \exp(-E_{\text{des}}/kT)$, where E_{des} (the isosteric heat of adsorption) is the difference between the potential energies of a molecule in the gaseous and adsorbed states. In fig. 10 this situation is reflected by the straight line at sufficiently low temperatures. The activation energy of long-range diffusion, as obtained from the slope of this line, is equal to 27 kJ/mol and, as to be expected, coincides with literature data for the heat of adsorption [106].

With further increasing temperature, however, molecular concentration in the intercrystalline space is likewise increasing so that mutual encounters of the molecules become more and more probable (bulk diffusion, insert on top). Eventually, the effective mean free path coincides with that in the gas phase, becoming inversely proportional to the gas phase pressure and hence to p_{inter}. As a consequence, the increase of p_{inter} with increasing temperature is compensated by the corresponding decrease of λ_{eff} and hence of D_{inter} , so that now $D_{\text{long-range}} = p_{\text{inter}} D_{\text{inter}}$ is only slightly increasing with the temperature, following the $T^{1/2}$ dependence of the thermal velocity.

A quantitative analysis [103], based on the adsorption isotherms and the intercrystalline porosity, yielded the remarkable result that a satisfactory fit between the experimental data and the estimates of $D_{\text{long-range}} = p_{\text{inter}} D_{\text{inter}}$ following eqs. (10) and (11) did only lead to coinciding results for tortuosity factors τ differing under the conditions of Knudsen diffusion (low temperatures) and bulk-diffusion (high temperatures) by a factor of at least 3. Similar results have most recently been obtained by dynamic Monte Carlo simulations [107-110]. In ref. [111] it is shown that the increase in the tortuosity factor as introduced by eq. (11) under the conditions of Knudsen diffusion may be attributed to the fact that with increasing tortuosity subsequent jumps are more and more anti-correlated, i.e. that any jump tends to counteract the displacement by the preceding one.

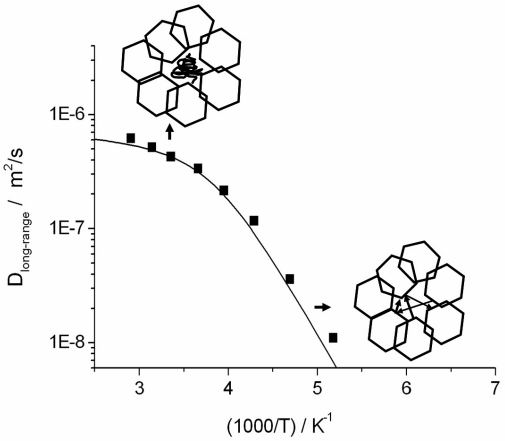

Fig. 10. Temperature dependence of the coefficient of long-range self-diffusion of ethane measured by PFG NMR in a bed of crystallites of zeolite NaX (points) and comparison with the theoretical estimate (line). The theoretical estimate is based on the sketched models of prevailing Knudsen diffusion (low temperatures, molecular trajectory consists of straight lines connecting the points of surface encounters) and gas phase diffusion (high temperatures, mutual collisions of the molecules lead to the Brownian-type of trajectories in the intercrystalline space).

It should be mentioned that - if technically applied as formed pellets - transport limitation may be due to both intracrystalline zeolitic diffusion as considered in section 2.1, and long-range diffusion as just considered. Denoting the mean radii of the crystallites and of the pellets by r_C and r_P, repectively, the respective time constants result to be $\tau_C = r_C^2/(15D_{\text{intra}})$ and $\tau_P = r_P^2/(15D_{\text{long-range}})$ [9, 112, 113]. Hence, being able to directly determine both D_{intra} and $D_{\text{long-range}}$, PFG NMR provides a straightforward means to explore the governing transport mechanism under technical application. In the case of FCC (fluid catalytic cracking) catalysts, being among the commercially most attractive zeolite catalyst at all [3], in this way it could be shown that - at least for the investigated, industrially used catalysts - the intracrystalline transport resistance was of no influence on the overall process, just in contrast to long-range ("intra-pellet") diffusion [114, 115].

4.2 Diffusion in Mesopores

In contrast to the just considered case of long-range-diffusion in beds of nanoporous particles, mass transfer within the pore network of monolithic compounds may occur both on the pore surface and in the pore volume. Molecular exchange between these two states of mobility may occur anywhere within the pore system, being completely uncorrelated with the respective diffusion paths. As a consequence, eq. (9) is

unrestrictedly applicable to describing "long-range" diffusion in the pore space. One obtains

$$D_{\text{long-range}} = p_{\text{surface}} D_{\text{surface}} + p_{\text{gas}} D_{\text{gas}} \qquad (12)$$

with $p_{\text{surface(gas)}}$ and $D_{\text{surface(gas)}}$ denoting the relative number of molecules on the pore surface (in the gas phase) and their diffusivities. Since the magnitudes of p_{gas} and D_{gas} may be calculated from the adsorption isotherm and the pore geometry [102, 116-118], with these data, due to $p_{\text{surface}} = 1 - p_{\text{gas}}$, the surface diffusivity D_{surface} may be calculated from the experimentally accessible long-range diffusivities.

Fig. 11 shows the results of this type of investigations with a sample of porous silicon [119], consisting of an array of parallel channel pores of 3.6 nm diameter with cyclohexane and acetone as probe molecules [120-122]. The measurements have been performed at room temperature. By connecting the sample volume to a gas reservoir with the probe molecules under study, sample loading could be easily varied by simply varying the pressure. A relative pore filling of $\theta \approx 0.5$ corresponds to about one monolayer of molecules adsorbed on the pore wall.

As a remarkable feature, for both sorbates under study, fig. 11 exhibits a most pronounced concentration dependence of the diffusivity. The fact that the diffusivity increases rather than decreases with increasing loading indicates that this dependence is not caused by a mutual molecular hindrance on the surface since in this case the reverse behaviour should be observed. Instead, one has to argue that the observed behaviour is a consequence of the guest-host rather than of the guest-guest interaction. In fact, one may imply that any surface heterogeneity tends to direct the first

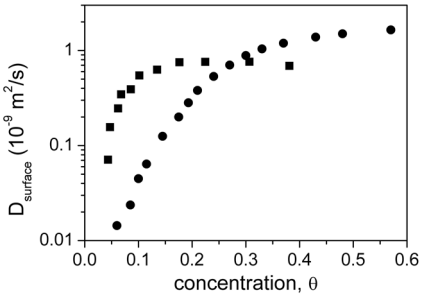

Fig. 11. The surface diffusion coefficient D_{surface} of cyclohexane (squares) and acetone (circles) in porous silicon with 3.6 nm mean pore diameter at pore loadings up to about one monolayer. The measurements were performed at T=297 K.

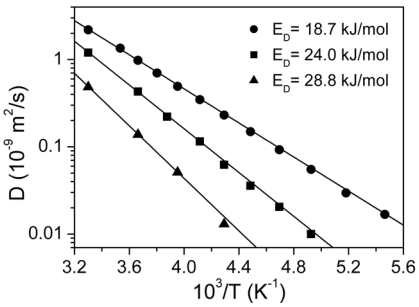

Fig. 12. The Arrhenius plots of the self-diffusion coefficients of acetone in porous silicon with 3.6 nm pore diameter at different pore concentrations $\theta = 0.6$ (circles), $\theta = 0.27$ (squares), and $\theta = 0.18$ (triangles). The solid lines show the fits to the experimental data using the Arrhenius relation $D \propto \exp(-E_D / RT)$ with the activation energies for diffusion E_D indicated in the figure.

molecules towards the strongest adsorption sites. Consequently, with increasing loading, sites with decreasing adsorption energies shall be occupied which results in a steadily decreasing average effective activation energy of diffusion [54].

This supposition is confirmed by the observed temperature dependences shown in fig. 12: In complete agreement with the predicted behaviour, the slope of the Arrhenius plots of the diffusivities decreases with increasing loading.

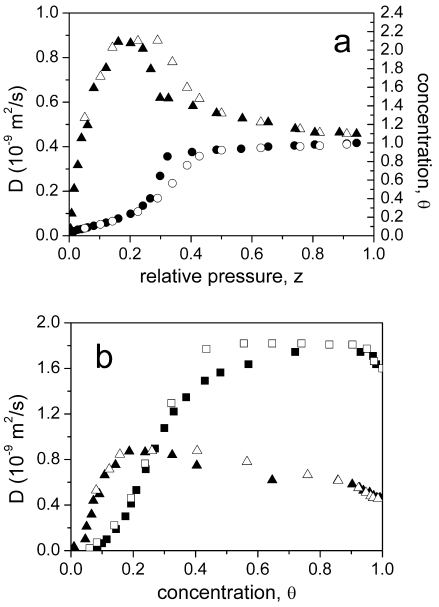

Fig. 13. (a) The adsorption-desorption isotherm (circles, right axis) and the self-diffusion coefficients D (triangles, left axis) for cyclohexane in porous silicon with 3.5 nm pore diameter as a function of the relative vapour pressure $z = p/p_S$, where p_S is the saturated vapour pressure. (b) The self-diffusion coefficients D for acetone (squares) and cyclohexane (triangles) as a function of the concentration θ of molecules in pores measured on the adsorption (open symbols) and the desorption (filled symbols) branches.

The experimental arrangement chosen in these studies allows monitoring the diffusion processes during adsorption hysteresis. Adsorption hysteresis is the phenomenon of history-dependent adsorption and describes the effect that, in addition to the pressure, the concentration also depends on whether the given pressure has been attained from lower values (i.e. on the "adsorption branch") or from higher values (the "desorption branch"). Irrespective of its great technical relevance for porosimetry [123] and the fact that the phenomenon of adsorption hysteresis is known over several decades already, its microscopic origin is still controversially discussed [124-128]. Owing to the PFG NMR data shown in fig. 13, now for the first time also information about the inherent diffusivities may be involved in this discussion. For cyclohexane as a probe molecule, fig. 13a shows both the total amount adsorbed and the respective diffusivity as a function of the pressure applied. In parallel with the amount adsorbed, also the diffusivities are found to differ on the adsorption and desorption branches for one and the same pressure. Even more interestingly, fig. 13 b shows the diffusivities on the adsorption and desorption branches as a function of the respective loadings. In addition to cyclohexane (redrawn from fig. 13 a), fig. 13 b also displays the data for acetone. As a most remarkable result, in both cases the diffusivities on the adsorption and desorption branches notably differ from each other for one and the same loading. This experimental finding strongly suggests that the differences in the adsorption and desorption branches are associated with differences in molecular arrangement and dynamics, which appear in the different diffusivities.

Following these first studies of molecular diffusion during hysteresis, we have also started to explore experimentally the consequences of hysteresis on sorption kinetics. As an example, fig. 14 shows the normalized curves of concentration equilibration (the "uptake curves") of cyclohexane in Vycor porous glass during the enhancement of the relative pressure $z = p/p_s$ (with p_s denoting the saturated vapour pressure) from 0.4 to 0.48 (top) and from 0.6 to 0.65 (bottom) [129]. As well indicated are the uptake curves resulting from the appropriate solution of Fick's law, i.e. by implying diffusion-controlled uptake. The diffusivity used in this estimate is that obtained by PFG NMR measurements.

For the pressure step $z = 0.4 \rightarrow 0.48$ excellent agreement is obtained. Hence, transient uptake measurements and self-diffusion measurements are found to lead to identical results. For the pressure step $z = 0.6 \rightarrow 0.65$, however, there is a remarkable difference between the measured uptake and the theoretical curve, estimated again by assuming diffusion-controlled uptake with a diffusivity as determined by PFG NMR. While in its first part the uptake curve follows the expected behaviour, with further loading the increase in molecular uptake is found to be notably behind the rate expected from molecular mobility.

In detailed studies over a series of pressure steps this deviation could be unambiguously attributed to the effect of adsorption hysteresis [129]. While during the pressure step $z = 0.4 \rightarrow 0.48$ the host-guest system was still in the pre-hysteresis range of complete reversibility, the second pressure step shown in fig. 14 was performed within the hysteresis loop. Here the host-guest system is known to assume metastable states. As a consequence, the new equilibrium state corresponding to the enhanced sorbate pressure has to be attained not only by mass transfer from outside. Rather it turns out to be limited by the relaxation of the system within a hierarchy of metastable states with decreasing free energy. In fact, the rate constant of this process is continuously increasing so that in the range of hysteresis genuine equilibrium should never be obtained [130].

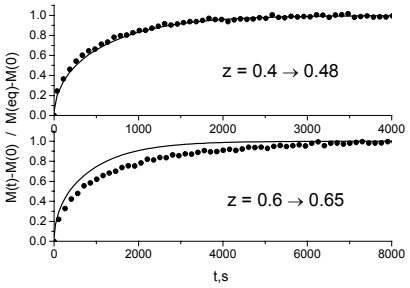

Fig. 14. Normalized concentration equilibration curves (circles) measured during adsorption of cyclohexane in Vycor porous glass beyond (upper figure) and in (lower figure) the region of the hysteresis. The pressure steps are indicated in the figures. The lines show the expected relaxation within the model of diffusion-controlled equilibration.

With the present study, for the first time an intriguing feature of the internal dynamics of mesoscalic systems, so far only treated by molecular modelling or mean-filed approaches [124-130] or forecasted from the loop of the adsorption isotherms, has been made accessible to direct experimental observation. Correlating these new experimental options with the findings of the theoretical treatment of these phenomena is among the primary topics of our future research.

5. Conclusion

Studying molecular diffusion under confinement by nanoporous host systems is a really interdisciplinary task. It has to be based on the availability of well-characterized porous materials and there is no doubt that the wealth of phenomena observable is intimately related to the abundance of materials applicable for this purpose. Fortunately, most recent progress in the field of synthesis has provided us with a multitude of highly sophisticated materials whose investigation will remain a challenging task over the next couple of years [131].

Simultaneously, the special conditions given by the properties of the new materials represent a permanent stimulus for the accomplishment of old and for the introduction of new measuring techniques. In the present contribution, the particular advantages of pulsed field gradient NMR and of interference and IR microscopy as microscopic measuring techniques for unveiling the peculiarities of molecular diffusion in nanoporous materials have been illustrated.

Most remarkably, diffusion studies by these microscopic techniques have been shown to serve as sensitive tools for the structural characterization of these novel materials, in many cases complementary to the more customary characterization methods like diffraction techniques and the different versions of (optical, electron, atomic force, tunnel...) microscopy.

Many of the transport phenomena predicted or already observed in the nanoporous materials under study are indispensably correlated with general theoretical concepts of molecular dynamics in mesoscopic systems. In this way, experimental findings and novel theoretical concepts will ensure mutual stimulation. As examples, we have considered the phenomenon of single-file diffusion as a process of high mutual correlation, the occurrence of anomalous diffusion in hierarchical pore networks and the establishment of metastable states during sorption hysteresis.

Nanoporous materials are in the very centre of many industrial processes, with mass separation and mass conversion as the most prominent representatives. In all these applications, mass transfer is among the rate-determining processes. Quantitation of the different diffusion resistances may therefore become a primary task for the design of materials of high technical performance. Novel concepts of pore design, including the formation of hierarchical pore structures, will lead to new generations of transport-optimized nanoporous materials.

Thus, stimulated by fundamental questions of dynamics in mesoscopic systems and the demand raised by multifold technical applications, studying molecular diffusion under nanoporous confinement has all potentials for maintaining its attractiveness for future research.

Acknowledgement: The results presented in this contribution are mainly based on experimental studies performed in the Department of Interface Physics of the Leipzig University. I am obliged to all my colleagues, co-workers and students for their contributions to these investigations. I particularly appreciate the cooperation by Petrik Galvosas, whom we owe the present, high level in the PFG NMR technique, to Sergey Vasenkov, who has significantly contributed to the development of interference microscopy and IR microscopy in our group, and to Rustem Valiullin for combining PFG

NMR with the in-situ pressure variation and all its options for studying surface diffusion and hystereses. I acknowledge the excellent conditions for national and international cooperation within the International Research Training Group "Diffusion in Porous Materials" and the International Research Group "Diffusion in Zeolites", jointly sponsored by DFG (Germany), NWO (Netherlands), CNRS (France) and EPSRC (UK), as well as in the collaborative initiatives TROCAT, INSIDE-PORES and INDENS under the auspices of the European Community.

References

[1] A. Fick, Ann. Phys. Chem. 94 (1855) 59.
[2] A. Einstein, Ann. Phys. 17 (1905) 549.
[3] J. Weitkamp, L. Puppe, Catalysis and Zeolites, Springer, Berlin Heidelberg, 1999.
[4] G. Ertl, H. Knötzinger, J. Weitkamp, Handbook of Heterogeneous Catalysis, Wiley-VCH, Chichester, 1997.
[5] J. Caro, M. Noack, P. Kölsch, R. Schäfer, Microporous Mesoporous Mater. 38 (2000) 3.
[6] D.M. Ruthven, S. Farooq, K.S. Knaebel, Pressure Swing Adsorption, VCH, New York, 1994.
[7] P.T. Callaghan, Principles of NMR Microscopy, Clarendon Press, Oxford, 1991.
[8] R. Kimmich, NMR Tomography, Diffusometry, Relaxometry, Springer, Berlin, 1997.
[9] J. Kärger, D.M. Ruthven, Diffusion in Zeolites and Other Microporous Solids, Wiley & Sons, New York, 1992.
[10] J. Kärger, H. Pfeifer, W. Heink, Advances in Magn. Reson. 12 (1988) 2.
[11] W.S. Price, Australian Journal of Chemistry 56 (2003) 855.
[12] P. Stilbs, Prog. Nucl. Magn. Reson. Spectrosc. 19 (1987) 1.
[13] B. Blümich, NMR Imaging of Materials, Clarendon Press, Oxford, 2000.
[14] K.H. Hausser, H.R. Kalbitzer, NMR für Mediziner und Biologen, Springer, Berlin, 1989.
[15] R.M. Cotts, Nature 351 (1991) 443.
[16] J. Kärger, W. Heink, J. Magn. Reson. 51 (1983) 1.
[17] J. Kärger, J. Caro, J. Chem. Soc. Faraday Trans. I 73 (1977) 1363.
[18] H. Pfeifer, Phys. Reports 26 (1976) 293.
[19] C. Baerlocher, W.M. Meier, D.H. Olson, Atlas of Zeolite Framework Types, 5 ed., Elsevier, Amsterdam, 2001.
[20] J. Weitkamp, H.G. Karge, H. Pfeifer, W. Hölderich, *Zeolites and Related Microporous Materials: State of the Art 1994*, Elsevier, Amsterdam, 1994.
[21] S.M. Auerbach, K.A. Carrado, P.K. Dutta, Handbook of Zeolite Science and Technology, Marcel Dekker, New York, 2003.
[22] J. Kärger, Adsorption-J. Int. Adsorpt. Soc. 9 (2003) 29.
[23] D.M. Ruthven, M.F.M. Post, in H. van Bekkum, E.M. Flanigen, J.C. Jansen (Eds.), Introduction to Zeolite Science and Practice, Elsevier, Amsterdam, 2001.

[24] D. Prinz, L. Riekert, Ber. Bunsenges. Phys. Chem. 90 (1986) 413.
[25] M. Bülow, A. Micke, Z. Phys. Chem. 189 (1995) 195.
[26] U. Schemmert, J. Kärger, J. Weitkamp, Microporous Mesoporous Mater. 32 (1999) 101.
[27] U. Schemmert, J. Kärger, C. Krause, R.A. Rakoczy, J. Weitkamp, Europhys. Lett. 46 (1999) 204.
[28] O. Geier, S. Vasenkov, E. Lehmann, J. Kärger, U. Schemmert, R.A. Rakoczy, J. Weitkamp, J. Phys. Chem. B 105 (2001) 10217.
[29] E. Lehmann, C. Chmelik, H. Scheidt, S. Vasenkov, B. Staudte, J. Kärger, F. Kremer, G. Zadrozna, J. Kornatowski, J. Amer. Chem. Soc. 124 (2002) 8690.
[30] J. Kärger, S. Vasenkov, in F. Laeri, F. Schüth, U. Simon, M. Wark (Eds.), Host-Guest Systems Based on Nanoporous Crystals, Wiley-VCH, Weinheim, 2003.
[31] J. Kärger, H. Pfeifer, in A. Pines, A. Bell (Eds.), NMR Techniques in Catalysis, Marcel Dekker, New York, 1994, p. 69.
[32] P.P. Mitra, P.N. Sen, L.M. Schwartz, Phys. Rev. B 47 (1993) 8565.
[33] P.P. Mitra, P.N. Sen, L.M. Schwartz, P. Ledoussal, Phys. Rev. Lett. 68 (1992) 3555.
[34] O. Geier, R.Q. Snurr, F. Stallmach, J. Kärger, J. Chem. Phys. 120 (2004) 1.
[35] S. Vasenkov, J. Kärger, Microporous Mesoporous Mat. 55 (2002) 139.
[36] S. Vasenkov, W. Böhlmann, P. Galvosas, O. Geier, H. Liu, J. Kärger, J. Phys. Chem. B. 105 (2001) 5922.
[37] J. Kärger, D.M. Ruthven, Zeolites 9 (1989) 267.
[38] C.E.A. Kirschhock, R. Ravishankar, L. Van Looveren, P.A. Jacobs, J.A. Martens, J. Phys. Chem. B 103 (1999) 4972.
[39] C.E.A. Kirschhock, R. Ravishankar, F. Verspeurt, P.J. Grobet, P.A. Jacobs, J.A. Martens, J. Phys. Chem. B 103 (1999) 4965.
[40] J.R. Agger, N. Hanif, C.S. Cundy, A.P. Wade, S. Dennison, P.A. Rawlinson, M.W. Anderson, J. Am. Chem. Soc. 125 (2003) 830.
[41] P. Kortunov, C. Chmelik, J. Kärger, R.A. Rakoczy, D.M. Ruthven, Y. Traa, S. Vasenkov, J. Weitkamp, Adsorption (2005) in press.
[42] P. Kortunov, S. Vasenkov, C. Chmelik, J. Karger, D.M. Ruthven, J. Wloch, Chemistry of Materials 16 (2004) 3552.
[43] D. Ben-Avraham, S. Havlin, Diffusion and Reaction in Fractals and Disordered Systems, University Press, Cambridge, 2000.
[44] G.H. Weiss, R.J. Rubin, Adv. Chem. Phys. 52 (1983) 363.
[45] J. Kärger, H. Spindler, J. Am. Chem. Soc. 113 (1991) 7571.
[46] M. Appel, G. Fleischer, J. Kärger, F. Fujara, S. Siegel, Europhys. Lett. 34 (1996) 483.
[47] I.Y. Chang, F. Fujara, B. Geil, G. Hinze, H. Sillescu, A. Tolle, J. Non-Cryst. Solids 172 (1994) 674.
[48] R. Kimmich, W. Unrath, G. Schnur, E. Rommel, J. Magn. Reson. 91 (1991) 136.
[49] M. Ylihautala, J. Jokisaari, E. Fischer, R. Kimmich, Phys. Rev. E. 57 (1998) 6844.
[50] D. Avnir, D. Farin, P. Pfeifer, J. Colloid Interface Sci. 103 (1985) 112.

[51] A. Bunde, S. Havlin, Fractals in Science, Springer, Berlin, 1995.
[52] A. Bunde, S. Havlin, Fractals and Disordered Systems, Springer, Berlin, 1996.
[53] P. Bräuer, S. Fritzsche, J. Kärger, G.M. Schütz, S. Vasenkov, in R. Haberlandt, D. Michel, A. Pöppl, R. Stannarius (Eds.), Molecules in Interaction with Surfaces and Interfaces, Springer, Berlin, 2004, p. 511.
[54] K.W. Kehr, K. Mussawisade, T. Wichmann, in J. Kärger, P. Heitjans, R. Haberlandt (Eds.), Diffusion in Condensed Matter, Vieweg/Springer, Braunschweig, 1998, p. 265.
[55] P.A. Fedders, Phys. Rev. B 17 (1978) 40.
[56] J. Kärger, Phys. Rev. E 47 (1993) 1427.
[57] J. Kärger, Phys. Rev. A 45 (1992) 4173.
[58] L. Riekert, Adv. Catal. 21 (1970) 281.
[59] J. Kärger, M. Petzold, H. Pfeifer, S. Ernst, J. Weitkamp, J. Catal. 136 (1992) 283.
[60] A.P.J. Jansen, S.V. Nedea, J.J. Lukkien, Phys. Rev. E 67 (2003) 046707.
[61] S.V. Nedea, A.P.J. Jansen, J.J. Lukkien, P.A.J. Hilbers, Phys. Rev. E. 65 (2002) 0066701.
[62] S.V. Nedea, A.P.J. Jansen, J.J. Lukkien, P.A.J. Hilbers, Physical Review E 66 (2002) 066705.
[63] A.P.J. Jansen, S.V. Nedea and J.J. Lukkien, Phys. Rev. E 67 (2003) 036104.
[64] C. Rödenbeck, J. Kärger, K. Hahn, Phys. Rev. 55 (1997) 5697.
[65] C. Rödenbeck, J. Kärger, K. Hahn, Ber. Bunsen-Ges. Phys. Chem. Chem. Phys. 102 (1998) 929.
[66] C. Rödenbeck, J. Kärger, K. Hahn, Phys. Rev. E. 57 (1998) 4382.
[67] C. Rödenbeck, J. Kärger, H. Schmidt, T. Rother, M. Rödenbeck, Phys. Rev. E 60 (1999) 2737.
[68] P.H. Nelson, S.M. Auerbach, J. Chem. Phys. 110 (1999) 9235.
[69] P.H. Nelson, S.M. Auerbach, Chem. Eng. J. 74 (1999) 43.
[70] C. Rödenbeck, J. Kärger, J. Chem. Phys. 110 (1999) 3970.
[71] S. Vasenkov, J. Kärger, Physical Review E 66 (2002) 052601
[72] P. Adhangale, D. Keffer, Sep. Sci. Technol. 38 (2003) 977.
[73] P. Demontis, J.G. Gonzalez, G.B. Suffritti, A. Tilocca, J. Am. Chem. Soc. 123 (2001) 5069.
[74] J.M.D. MacElroy, S.H. Suh, Microporous Mesoporous Mat. 48 (2001) 195.
[75] D.S. Sholl, C.K. Lee, J. Chem. Phys. 112 (2000) 817.
[76] D.S. Sholl, K.A. Fichthorn, Physical Review A. 55 (1997) 7753.
[77] K. Hahn, J. Kärger, Journal of Physical Chemistry. 100 (1996) 316.
[78] S.Y. Bhide, S. Yashonath, J. Phys. Chem. B. 104 (2000) 11977.
[79] S.Y. Bhide, S. Yashonath, J. Am. Chem. Soc. 125 (2003) 7425.
[80] Z. Kapinski, S.N. Ghandi, W.M.H. Sachtler, J. Catal. 141 (1993) 337.
[81] G.D. Lei, W.M.H. Sachtler, J. Catal. 140 (1993) 601.
[82] G.D. Lei, B.T. Carvill, W.M.H. Sachtler, Applied Catalysis A-General. 142 (1996) 347.
[83] C. Rödenbeck, J. Kärger, K. Hahn, W. Sachtler, J. Catal. 183 (1999) 409.
[84] F.J.M.M. de Gauw, J. van Grondelle, R.A. van Santen, J. Catal. 204 (2001) 53.

[85] C. Rödenbeck, J. Kärger, K. Hahn, J. Catal. 157 (1995) 656.
[86] C. Rödenbeck, J. Kärger, K. Hahn, J. Catal. 176 (1998) 513.
[87] V. Gupta, S.S. Nivarthi, A.V. McCormick, H.T. Davis, Chem. Phys. Lett. 247 (1995) 596.
[88] K. Hahn, J. Kärger, V. Kukla, Phys. Rev. Lett. 76 (1996) 2762.
[89] V. Kukla, K. Hahn, J. Kärger, in N.C.U. Press (Eds.), Rozwadowski, M., Torun, 1995, p. 110.
[90] V. Kukla, J. Kornatowski, D. Demuth, I. Gimus, H. Pfeifer, L.V.C. Rees, S. Schunk, K.K. Unger, J. Kärger, Science. 272 (1996) 702.
[91] T. Meersmann, J.W. Logan, R. Simonutti, S. Caldarelli, A. Comotti, P. Sozzani, L.G. Kaiser, A. Pines, J. Phys. Chem. A. 104 (2000) 11665.
[92] H. Jobic, K. Hahn, J. Kärger, M. Bee, A. Tuel, M. Noack, I. Girnus, G.J. Kearley, Journal of Physical Chemistry B. 101 (1997) 5834.
[93] K. Hahn, J. Kärger, J. Phys. Chem. 102 (1998) 5766.
[94] E. Lehmann, S. Vasenkov, J. Kärger, G. Zadrozna, J. Kornatowski, J. Chem. Phys. 118 (2003) 6129.
[95] E. Lehmann, S. Vasenkov, J. Kärger, G. Zadrozna, J. Kornatowski, Ö. Weiss, F. Schüth, J. Phys. Chem. B 107 (2003) 4685.
[96] J. Kornatowski, G. Zadrozna, J. Wloch, M. Rozwadowski, Langmuir 15 (1999) 5863.
[97] J. Kornatowski, G. Zadrozna, M. Rozwadowski, B. Zibrowius, F. Marlow, J.A. Lercher, Chem. Mater. 13 (2001) 4447.
[98] B.V. Padlyak, J. Kornatowski, G. Zadrozna, M. Rozwadowski, A. Gutsze, J. Phys. Chem. A 104 (2000) 11837.
[99] B. Newling, S.N. Batchelor, Journal of Physical Chemistry B 107 (2003) 12391.
[100] K.I. Momot, P.W. Kuchel, Concepts in Magnetic Resonance Part A 19A (2003) 51.
[101] C. Meier, W. Dreher, D. Leibfritz, Magnetic Resonance in Medicine 50 (2003) 510.
[102] J. Kärger, M. Kocirik, A. Zikanova, J. Colloid Interface Sci. 84 (1981) 240.
[103] O. Geier, S. Vasenkov, J. Kärger, J. Chem. Phys. 117 (2002) 1935.
[104] W. Jost, Diffusion in Solids, Liquids and Gases, Academic Press, New York, 1960.
[105] C.N. Satterfield, Mass Transfer in Heterogeneous Catalysis, M.I.T. Press, Cambridge, Massachusetts and London, England, 1970.
[106] J.A. Dunne, M.B. Rao, S. Sircar, R.J. Gorte, A.L. Myers, Langmuir 12 (1996) 5896.
[107] K. Malek, M.O. Coppens, Phys. Rev. Lett. 87 (2001) 125505.
[108] K. Malek, M.O. Coppens, Colloid Surf. A 206 (2002) 335.
[109] K. Malek, M.O. Coppens, J. Chem. Phys. 119 (2003) 2801.
[110] V.N. Burganos, J. Chem. Phys. 109 (1998) 6772.
[111] J.M. Zalc, S.C. Reyes, E. Iglesia, Chem. Engin. Sci. 59 (2004) 2947.
[112] N.Y. Chen, T.F. Degnan, C.M. Smith, Molecular Transport and Reaction in Zeolites, VCH , New York, 1994.

[113] F. Keil, Diffusion und Chemische Reaktion in der Gas/Feststoff-Katalyse, Springer , Berlin, 1999.
[114] J. Kärger, S. Vasenkov, Micro. Mesopor. Mater. (2005) in press.
[115] P. Kortunov, S. Vasenkov, J. Karger, M.F. Elia, M. Perez, M. Stocker, G.K. Papadopoulos, D. Theodorou, B. Drescher, G. McElhiney, B. Bernauer, V. Krystl, M. Kocirik, A. Zikanova, H. Jirglova, C. Berger, R. Glaser, J. Weitkamp, E.W. Hansen, Magnetic Resonance Imaging 23 (2005) 233.
[116] F. Rittig, C.G. Coe, J.M. Zielinski, J. Am. Chem. Soc. 124 (2002) 5264.
[117] F. Rittig, C.G. Coe, J.M. Zielinski, J. Phys. Chem. B 107 (2003) 4560.
[118] F. Rittig, T.S. Farris, J.M. Zielinski, AIchE Journal 50 (2004) 589.
[119] V. Lehmann, R. Stengl, A. Luigart, Materials Science and Engineering B - Solid State Materials for Advanced Technology 69 (2000) 11.
[120] R. Valiullin, P. Kortunov, J. Kärger, V. Timoshenko, J. Chem. Phys. 120 (2004) 11804.
[121] R. Valiullin, P. Kortunov, J. Kärger, V. Timoshenko, J. Phys. Chem. B 109 (2005) 5746.
[122] J. Kärger, R. Valiullin, S. Vasenkov, New Journal of Physics 7 (2005) 1.
[123] F. Schüth, K.S.W. Sing, J. Weitkamp, Handbook of Porous Solids, Wiley-VCH, Weinheim, 2002.
[124] L. Sarkisov, P.A. Monson, Langmuir. 16 (2000) 9857.
[125] E.A. Ustinov, D.D. Do, J.Chem.Phys. 120 (2004) 9769.
[126] E. Kierlik, P.A. Monson, M.L. Rosinberg, L. Sarkisov, G. Tarjus, Phys.Rev.Letts. 87 (2001) 055701.
[127] B. Coasne, A. Grosman, C. Ortega, M. Simon, Phys. Rev. Lett. 88 (2002) 256102.
[128] D. Wallacher, N. Kunzner, D. Kovalev, N. Knorr, K. Knorr, Phys. Rev. Lett. 92 (2004) 195704.
[129] R. Valiullin, J. Kärger, P.A. Monson, Poster abstract in this volume.
[130] H.-J. Woo, P.A. Monson, Phys. Rev. E 67 (2003) 041207.
[131] F. Laeri, F. Schüth, U. Simon, M. Wark, Host-Guest Systems Based on Nanoporous Crystals, Wiley-VCH, Weinheim, 2003.